Nonlinear Spin–Orbit Interaction of Light in a Cold Rydberg Atom Medium

Lu Qin[1], Chao Hang[2], Weibin Li[3,4*], and Xingdong Zhao[1*]

[1]*School of Physics, Henan Normal University, Xinxiang 453007, China*
[2]*State Key Laboratory of Precision Spectroscopy, Institute of Quantum Science and Precision Measurement, East China Normal University, Shanghai 200241, China*
[3]*School of Physics and Astronomy, University of Nottingham, Nottingham NG7 2RD, United Kingdom*
[4]*Centre for the Mathematics and Theoretical Physics of Quantum Non-Equilibrium Systems, University of Nottingham, Nottingham NG7 2RD, United Kingdom*

(Received 15 January 2026; accepted manuscript online 13 April 2026)

We demonstrate that a nonlinear spin–orbit interaction (SOI) emerges in cold Rydberg atomic gases, where the orbital characteristics (spatial structure) of light fields become coupled to their polarization (spin). This SOI originates from the giant, spatially inhomogeneous nonlinear optical response arising from the strong, long-range interactions between Rydberg atoms. By extending the theoretical framework beyond the conventional paraxial approximation, we derive a light propagation equation that rigorously incorporates such inhomogeneous nonlinearity. Our study reveals that the SOI is driven by the gradient of the inhomogeneous nonlinear response and therefore vanishes in linear or homogeneous media. When two orthogonal light fields co-propagate, the SOI generates novel nonlinear energy transfer and pronounced structural deformation, which are not captured without considering the SOI or within the paraxial approximation. Furthermore, owing to its direct dependence on the gradient of the nonlocal nonlinearity, the SOI is inherently mode-dependent. As a consequence, the structural deformation becomes particularly significant for light fields with odd parity symmetry. Our investigation establishes novel pathways for exploring the nonlinear SOI and examining inhomogeneous nonlinear optical responses beyond the paraxial approximation in cold Rydberg atomic gases.

DOI: 10.1088/0256-307X/43/5/050303 CSTR: 32039.14.0256-307X.43.5.050303

1. Introduction. Spin–orbit (SO) effects of light have attracted growing interest recently, which describes the coupling between the polarization (spin) and wave trajectory of light fields.[1,2] The SO effect has initially been demonstrated in optical fibers, giving rise to optical ping-pong and Magnus effects.[1,3,4] These studies revealed the influence of the trajectory on the polarization, leading to rotations of Rytov–Vladimirsky–Berry–Chiao type and the formation of speckle patterns.[1] The SO effect has also been investigated in a layered locally isotropic medium, where it manifests as effective birefringence.[5–7] Moreover, SO coupling underlies the spin Hall effect of light,[8–14] which is highly sensitive to the polarization of incident light. This effect has enabled applications such as quantum weak measurement[15,16] and enhanced spin transport.[17] Several studies have focused on the SO effects in the paraxial regime.[18,19]

Beyond the paraxial regime, the coupling between photon spin and wave trajectory in the presence of inhomogeneous nonlinearities gives rise to spin–orbit interactions (SOIs).[18,20–23] These interactions emerge from the wave equation in inhomogeneous media and originate from symmetry breaking induced by spatial gradients of the optical response. The intrinsic SOI of light can ultimately be traced back to the spin-like properties of Maxwell's equations.[2,11,21] A key ingredient to produce SOI is a spatially inhomogeneous refractive index, which is typically found in optical waveguides,[24] photonic crystals,[20,25,26] and optical fibers.[27,28] However, the requirement of strong inhomogeneous nonlinearity has limited the study of SOIs mostly to solid-state systems, such as plasmonic slits,[16] photonic crystals,[29] non-paraxial beams,[30] random media,[31,32] and dielectric interfaces.[15] In these systems, the dynamics takes place on much shorter time scales and suffers from dissipation, which makes the SOI effect difficult to observe.[14] In contrast, cold atomic gases interacting with laser fields provide a promising platform for studying SOI.[33,34] When light is coupled to electronically high-lying Rydberg states,[35,36] strong and long-range interactions between Rydberg atoms can be mapped onto light fields through electromagnetically induced transparency (EIT),[37] generating dispersive nonlocal nonlinearity (NNL)[38,39] that is enhanced by four orders of magnitude compared to that of ground-state atomic systems.[40,41] Moreover, the degree of nonlocality of the nonlinearity can be flexibly tuned by modifying the blockade radius R_b and the beam waist radius R_0 of the optical field. However, whether SOIs can be induced in strongly nonlinear, nonlocal Rydberg media has not been studied.

In this work, we show the onset of SOI in an optical medium of cold Rydberg atomic gases. The SOI re-

*Corresponding authors. Email: weibin.li@nottingham.ac.uk; phyzhxd@gmail.com
© 2026 Chinese Physical Society and IOP Publishing Ltd. All rights, including for text and data mining, AI training, and similar technologies, are reserved.

lies on the giant nonlocal nonlinear optical response that is induced through strong nonlocal atom–atom interactions.[36,37] In the Maxwell equations, the strong nonlinearity generates a sizable non-paraxial effect, in which the refractive-index gradient couples light polarization and orbital motions, leading to SOI.[18] The refractive-index gradient acts as an external driving force, analogous to a gradient force.[21,42] We further show that the SOI can be significantly enhanced in elliptically polarized light fields consisting of weak and strong fields. When propagating in the Rydberg medium, the nonlinear SOI causes energy exchange between the strong and weak fields. Moreover, we illustrate that the SOI-induced deformation of the weak field depends sensitively on the orbital structure of the strong field.

2. Light Propagation beyond the Paraxial Approximation. In our setting, two linearly polarized light fields co-propagate along the z-direction in a cold Rydberg atomic gas, as shown in Fig. 1(a). Through EIT, the strong interactions between Rydberg atoms are mapped onto the light field, leading to a nonlocal nonlinear refractive index $\delta n(\boldsymbol{r})$. After adiabatically eliminating the atomic coherence,[37,43] the refractive index can be obtained as $n = n_0 + \delta n$, where the nonlocal nonlinear contribution takes the form $\delta n(\boldsymbol{r}_\perp) \approx \int \widetilde{\chi}^{(3)}\, \mathrm{d}^2\boldsymbol{r}'_\perp = A\int \left(R_\mathrm{b}^6 + |\boldsymbol{r}_\perp - \boldsymbol{r}'_\perp|^6\right)^{-1} \mathrm{d}^2\boldsymbol{r}'_\perp\, |\boldsymbol{E}(\boldsymbol{r}_\perp)|^2$ with $\boldsymbol{r}_\perp = (x, y)$, which has a soft-core spatial profile. Here, n_0 denotes the background refractive index (i.e., $n_0 = 1$), A is a parameter determined by the Rydberg state and the laser field, R_b is the soft-core radius,[43,44] and $\widetilde{\chi}^{(3)}$ is the nonlinear susceptibility [see Supplementary Materials (SM) for details on its relation to the refractive index]. An example of the nonlinear susceptibility is shown in Fig. 1(b), where $\widetilde{\chi}^{(3)}$ is significant within the soft-core radius R_b and becomes negligible outside this region.

Two important properties are found in the Rydberg-atom-induced optical response that are absent in local nonlinearity. First, under typical experimental conditions, the blockade radius R_b can be tuned over the range ∼3–20 μm by selecting different Rydberg states.[45] This length scale is compatible with the beam waist R_0, such that spatially nonlocal effects play an important role during propagation.[43] Depending on the relative magnitudes of R_b and R_0, the Rydberg atomic system exhibits different regimes of nonlocality. In the limit $R_\mathrm{b} \ll R_0$, it exhibits a local response, indicating that neither a spatially inhomogeneous refractive index nor the SOI effect occurs. In contrast, when $R_\mathrm{b} \gtrsim R_0$, it exhibits a nonlocal response, indicating that the refractive index becomes spatially inhomogeneous. Second, the optical response is giant in cold Rydberg atomic media.[46] As detailed in the SM, the nonlinear susceptibility can reach four orders of magnitude higher than that of local Kerr nonlinearities induced by EIT involving the electronically low-lying manifold.[47] Importantly, the Rydberg-induced NNL is dominated by the dispersive component, largely due to the long lifetimes of Rydberg states.[36]

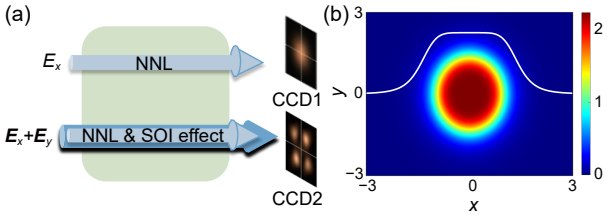

Fig. 1. (a) Light fields propagate through an optical medium. Linearly polarized light experiences the NNL, whereas in the presence of two polarized fields, both NNL and SOI affect the propagation dynamics. The two cases lead to different output patterns recorded by the CCD cameras. (b) The nonlocal nonlinear susceptibility $\widetilde{\chi}^{(3)}$ exhibits a soft-core spatial profile. The white solid line shows the cross-section at $y = 0$.

Previous investigations on light propagation in atomic gases have commonly relied on the paraxial approximation, which is suitable when the optical response is local and weak, that is, when the beam waist R_0 and the diffraction length kR_0^2 (where k is the wavenumber) are comparable. In this regime, the parabolic equation fails for two reasons. First, the term involving the second-order transverse derivative of the field envelope, $\nabla_\perp^2\boldsymbol{E}$, cannot fully capture diffraction effects, rendering the paraxial approximation insufficient. Second, the commonly adopted assumption $\nabla(\nabla\cdot\boldsymbol{E}) = 0$ no longer holds. To address these limitations, we extend the theoretical framework beyond the paraxial approximation. Starting from the Maxwell equations and using the nonparaxial approach (see SM for details of the derivation), the light field propagation is governed by the Helmholtz equation,[18,48–50]

$$\nabla^2\boldsymbol{E} + 2\nabla(\boldsymbol{E}\cdot\nabla\ln n) + \omega^2\epsilon\mu\boldsymbol{E} = 0\,, \tag{1}$$

where the second term on the left-hand side is responsible for the SOI, ϵ is the dielectric constant, and μ is the permeability constant.

We consider an elliptically polarized field of the form $\boldsymbol{E} = \exp(\mathrm{i}\omega n_0 z/c)\,\boldsymbol{E}_\perp(x, y, z)$, where the transverse component $\boldsymbol{E}_\perp = E_x\boldsymbol{e}_x + E_y\boldsymbol{e}_y$ consists of two linearly polarized light fields with amplitudes E_x and E_y. By going beyond the paraxial approximation,[1,4] the propagation of $\boldsymbol{E}_\perp$ is governed by a Schrödinger-like nonlinear equation,

$$\mathrm{i}\frac{\partial\boldsymbol{E}_\perp}{\partial z} = \mathcal{H}_0\boldsymbol{E}_\perp + \delta\mathcal{H}\,\boldsymbol{E}_\perp + \mathcal{H}_1\,, \tag{2}$$

where $\mathcal{H}_0 = -(2\kappa)^{-1}\nabla_\perp^2 - (\omega/c)\,[n(\boldsymbol{r}_\perp) - n_0]$ is the unperturbed Hamiltonian with $\kappa = \omega n_0/c$; $\delta\mathcal{H} = (2\kappa)^{-1}\mathcal{H}_0\mathcal{H}_0$ is a second-order correction Hamiltonian by the procedure of iteration; $\mathcal{H}_1 = -\nabla_\perp\left[\boldsymbol{E}_\perp\cdot\nabla_\perp\ln n(\boldsymbol{r}_\perp)\right]/\kappa$ couples polarization to the spatial structure of the optical field and corresponds to the SOI. To illustrate the SOI, the propagation equations for the two linearly polarized light fields are explicitly given by

$$\mathrm{i}\frac{\partial}{\partial z}\begin{pmatrix}E_x\\E_y\end{pmatrix} = \begin{pmatrix}\mathcal{H}_x & \mathcal{S}_{xy}\\ \mathcal{S}_{yx} & \mathcal{H}_y\end{pmatrix}\begin{pmatrix}E_x\\E_y\end{pmatrix}\,, \tag{3}$$

where the diagonal terms are $\mathcal{H}_\beta = \mathcal{H}_0 + \delta\mathcal{H} - \mathcal{S}_{\beta\beta}$ ($\beta = x, y$), and $\mathcal{S}_{\beta\beta'}$ ($\beta' = x, y$ and $\beta' \neq \beta$) denote the off-diagonal coupling terms. Due to the nonparaxial approximation, extra terms appear in the propagation equation,

namely, $\mathcal{S}_{\beta\bar{\beta}} = -\frac{1}{\kappa}\frac{\partial}{\partial\beta}\frac{\partial \ln n}{\partial\bar{\beta}}$ $(\bar{\beta} = \beta, \beta')$, which describe the SOI. It depends on the gradient of inhomogeneity of the refractive index $n(\boldsymbol{r}_\perp)$, i.e., $\delta n(\boldsymbol{r}_\perp)$, and induces coupling between the two fields, which is a defining feature of the SOI in inhomogeneous media. This coupling distinguishes it from the diagonal component $\mathcal{S}_{\beta\beta}$, which primarily induces a cross-Kerr dispersive effect wherein one light field is influenced by the intensity of the other. Crucially, the SOI arises from the combined effect of light intensity and nonlocal susceptibility, making its contribution significant even when the light field varies smoothly in space. This feature contrasts sharply with that in a local Kerr medium, where the SOI is negligible due to the spatially uniform susceptibility. However, the SOI is essential in Rydberg atomic media owing to their giant and nonlocal optical response. For convenience, we introduce dimensionless variables (beam waist R_0 and peak amplitude E_0) by scaling the transverse coordinates and field amplitudes as $\{x, y\} \to \{R_0 x, R_0 y\}$ and $\{E_x, E_y\} \to \{E_0\bar{E}_x, E_0\bar{E}_y\}$. In the following analysis, we consider typical parameters $R_0 = 3.5\,\mu\text{m}$ and $E_0 = 70\,\text{V/m}$.

3. Scaling of the SOI. The SOI is typically much weaker than the nonlocal nonlinear interaction contained in the Hamiltonian $\mathcal{H}_0$, making its effects difficult to isolate. To quantify its contribution, we first apply perturbation theory to determine the scaling of the SOI with the external field. Since gradient operations alter the spatial symmetries of both the light field and the refractive-index variation δn, the SOI is inherently sensitive to the beam profiles. In the perturbation calculation, we first consider the local density approximation $\delta n \approx A\left(|\bar{E}_x|^2 + |\bar{E}_y|^2\right)/R_\text{b}^6$, which is valid when the blockade radius R_b is much smaller than the width of the light field.[51,52] Assuming that the input light fields remain undeformed during propagation, we calculate the expectation values $\langle\mathcal{S}_{xx}\rangle = \int \bar{E}_x^*\,\mathcal{S}_{xx}\,\bar{E}_x\,\mathrm{d}^2\boldsymbol{r}_\perp$ and $\langle\mathcal{S}_{xy}\rangle = \int \bar{E}_x^*\,\mathcal{S}_{xy}\,\bar{E}_y\,\mathrm{d}^2\boldsymbol{r}_\perp$ using the input field as an ansatz. Specifically, we consider Hermite–Gaussian (HG) modes as the input fields,

$$\bar{E}_\beta = \bar{E}_\beta^0\, H_m\!\left(\frac{\sqrt{2}\,x}{w_0}\right) H_k\!\left(\frac{\sqrt{2}\,y}{w_0}\right)\exp\!\left[-\frac{x^2+y^2}{w_0^2}\right], \quad (4)$$

where $\bar{E}_\beta^0$ is the amplitude, $H_m(\cdot)$ denotes the Hermite polynomial of order m, and $\{m, k\}$ are the transverse mode indices.

Since δn is a spatially even function and the gradient operator changes spatial symmetries along the respective direction, the condition $\langle\mathcal{S}_{xy}\rangle \neq 0$ requires that the integral kernel in $\langle\mathcal{S}_{xy}\rangle$ be even with respect to both the x- and y-axes. In contrast, $\langle\mathcal{S}_{xx}\rangle$ is nonzero for all modes, as the kernel is always an even function. This mode dependence is a key consequence of the SOI. To elucidate this behavior, we vary the mode of the y-polarized light while fixing $\bar{E}_x$ to the HG00 mode, i.e., $m = k = 0$. We find that $\langle\mathcal{S}_{xx}\rangle \propto |\bar{E}_x^0\bar{E}_y^0|^2$, indicating a quadratic dependence on both $|\bar{E}_x^0|$ and $|\bar{E}_y^0|$. With the x-polarized mode fixed, the SOI exhibits a more sensitive dependence on the y-polarized light. Due to the different spatial symmetries of the x- and y-polarized fields, only the HG11 mode generates a nonzero SOI, with $\langle\mathcal{S}_{xy}\rangle \propto |\bar{E}_x^0||\bar{E}_y^0|^3$, whereas $\langle\mathcal{S}_{xy}\rangle$ vanishes for the HG00, HG01, and HG10 modes. Although the scaling is derived within the local density approximation, it remains valid in the nonlocal regime. In the latter case, the integration in the NNL affects the coefficient but not the scaling with the field.

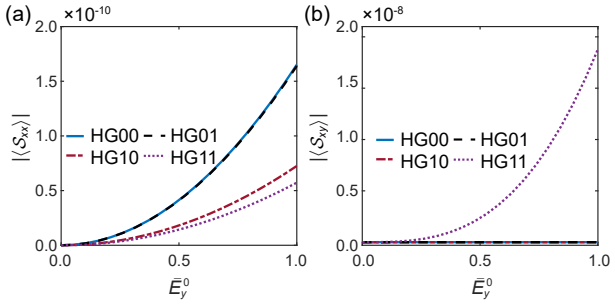

Fig. 2. Scaling of (a) $\langle\mathcal{S}_{xx}\rangle$ and (b) $\langle\mathcal{S}_{xy}\rangle$ as functions of $\bar{E}_y^0$. Panel (a) shows that $\langle\mathcal{S}_{xx}\rangle$ increases quadratically with $\bar{E}_y^0$. Panel (b) shows that the HG11 mode generates a significantly large SOI when $\bar{E}_y^0 \gg \bar{E}_x^0$, whereas the other modes lead to vanishing SOIs. The blue solid, black dashed, red dashed-dotted, and purple dotted lines correspond to the HG00, HG01, HG10, and HG11 modes, respectively. The parameters are $\bar{E}_x^0 = 0.01$, $w_0 = 1$, $A = 4.6 \times 10^{-4}$, and $R_\text{b} = 1$ (in unit of R_0).

Here, $\langle\mathcal{S}_{xy}\rangle$ scales linearly with $\bar{E}_x^0$ and cubically with $\bar{E}_y^0$, in contrast to the quadratic field dependence of $\langle\mathcal{S}_{xx}\rangle$. As a result, the two terms are comparable when the two fields have similar strengths. Exploiting their distinct scaling behaviors, the contribution of $\langle\mathcal{S}_{xy}\rangle$ can be significantly enhanced in an imbalanced regime with $\bar{E}_y^0 \gg \bar{E}_x^0$. In Figs. 2(a) and 2(b), we show the dependence of $\langle\mathcal{S}_{xx}\rangle$ and $\langle\mathcal{S}_{xy}\rangle$ on $\bar{E}_y^0$, respectively. The quadratic behavior of $\langle\mathcal{S}_{xx}\rangle$ with respect to $\bar{E}_y^0$ is shown in Fig. 2(a), where $\langle\mathcal{S}_{xx}\rangle \neq 0$ for all mode choices. In contrast, figure 2(b) shows that, due to spatial symmetry, $\langle\mathcal{S}_{xy}\rangle$ is nonzero for the HG11 mode and becomes significantly enhanced when $\bar{E}_y^0/\bar{E}_x^0 \geq 50$. Importantly, the perturbation results show that $\langle\mathcal{S}_{xy}\rangle$ is about two orders of magnitude larger than $\langle\mathcal{S}_{xx}\rangle$ when $\bar{E}_y^0 \sim 1 \gg \bar{E}_x^0$. To further compare the nonlinear and SOI effects, we calculate the maximum values of δn, $\mathcal{S}_{xx}$, and $\mathcal{S}_{xy}$ for the HG11 mode, which are 9.95×10^{-4}, 2.99×10^{-7}, and 2.57×10^{-5}, respectively. We see that the SOI is sizable compared to the nonlinearity.

4. SOI Driven Nonlinear Energy Transfer. Using the insight gained from the perturbation calculation, we will study the propagation dynamics in the field-imbalanced regime $\bar{E}_y^0 \gg \bar{E}_x^0$. To capture the rich SO effect, we extend beyond the perturbation calculation and solve the (2+1)-dimensional light propagation Eq. (2) numerically. We consider an initial state where $\bar{E}_x$ is a Gaussian mode, while $\bar{E}_y$ is an HG10 mode. We first examine a scenario in which the SOI is artificially excluded during propagation. Although this is not physically realizable, it allows us to isolate the role of the nonlinearity δn. The transverse intensity profiles at different propagation distances z are shown in Fig. 3(a). Initially, the x-polarized field deviates from the Gaussian mode and splits into two peaks

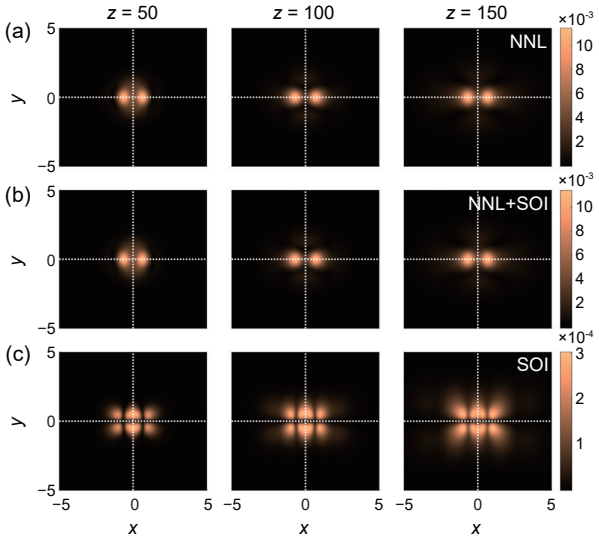

Fig. 3. Light-field intensity $|\bar{E}_x^0|$ at different propagation distances z. The initial fields $\bar{E}_x$ and $\bar{E}_y$ correspond to the HG00 and HG10 modes, respectively. In (a), the SOI is turned off, i.e., $\mathcal{S}_{xx} = \mathcal{S}_{xy} = 0$. In (b), the SOI is fully included in the simulation. Panel (c) shows the difference between the fields in (b) and (a), highlighting the SOI-induced modification of $\bar{E}_x$, which is relatively weak. The three columns show propagation distances at $z = 50$, 100, and 150. Other parameters are $\bar{E}_x^0 = 0.01$, $\bar{E}_y^0 = 1$, $w_0 = 1$, $A = 4.6 \times 10^{-4}$, and $R_b = 1$.

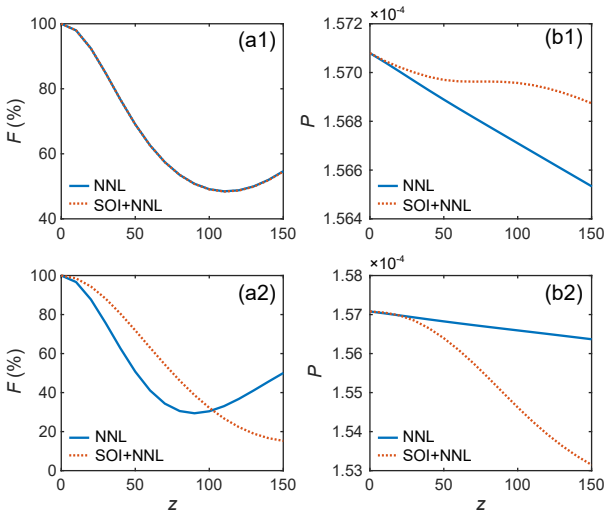

Fig. 4. (a1) and (a2) Mode-dependent fidelity of the field $\bar{E}_x$. (b1) and (b2) Mode-dependent power of the field $\bar{E}_x$. In (a1) and (b1), the y-polarized field $\bar{E}_y$ is prepared in the HG10 mode; in (a2) and (b2), $\bar{E}_y$ is prepared in the HG11 mode. The other parameters are the same as those shown in Fig. 3.

($z = 50$). The two peaks gradually separate from each other (see examples at $z = 100$ and $z = 150$), until $\bar{E}_x$ resembles the profile of the y-polarized field.[39] This is a direct consequence of the nonlinear interaction induced by the cross-Kerr effect. The y-polarized field $\bar{E}_y$ creates a guiding potential that confines the field $\bar{E}_x$ into the low-potential region (corresponding to the high-field-strength regime of the HG10 mode). As the HG10 mode is symmetric with respect to $x = 0$ and $y = 0$, the deformed $\bar{E}_x$ field exhibits the same symmetry. As shown in Fig. 3(a), the nonlinearity preserves the spatial symmetries of the field $\bar{E}_x$, despite its profile being altered. Moreover, the nonlinearity is determined jointly by $\bar{E}_x$ and $\bar{E}_y$. Since $\bar{E}_y^0$ is much larger than $\bar{E}_x^0$, the changes in $\bar{E}_x$ are negligible compared to those in $\bar{E}_y$ during propagation.

The simulation results including both nonlinearity and SOI are shown in Fig. 3(b). Based on the perturbative analysis of the SOI effect shown in Fig. 2, the contributions from both $\mathcal{S}_{xx}$ and $\mathcal{S}_{xy}$ are relatively small. Therefore, the profile of field $\bar{E}_x$ in Fig. 3(b) appears to be largely unchanged compared to the case with nonlinearity only. Although the difference between Figs. 3(a) and 3(b) appears subtle, a direct subtraction of the two fields shows that SOI slightly modifies the shape of the $\bar{E}_x$ field, as shown in Fig. 3(c). Notably, this modification affects larger areas as the light propagates in the medium.

To quantify the distortion of the x-polarized field induced by the SOI and nonlocal nonlinear interaction, we calculate the waveshape fidelity,[39] $F = P_0^{-1} P^{-1} \left| \int \bar{E}_x(z)\, \bar{E}_x^*(z=0)\, \mathrm{d}^2 \boldsymbol{r}_\perp \right|^2$, where $P = \int |\bar{E}_x(z)|^2\, \mathrm{d}^2 \boldsymbol{r}_\perp$ is the power at propagation distance z, and P_0 is the initial power. The fidelity F describes the overlap of the field $\bar{E}_x$ with its initial profile. During propagation in the Rydberg medium, the fidelity first decreases rapidly before a slight recovery when $z > 100$, as shown by the blue curve in Fig. 4(a1). Since the SOI-induced modification is relatively weak, the fidelities obtained with and without SOI are nearly identical, leading to an almost perfect overlap of the two curves in Fig. 4(a1).

In contrast, the beam power P shows a more distinct change due to SOI, as depicted in Fig. 4(b1). In the presence of nonlocal nonlinear interaction alone, the power of the x-polarized field decreases, as indicated by the blue solid curve. When the SOI is included, however, the power of the x-polarized field increases, resulting in a higher overall power (red dashed curve) compared to the nonlinearity-only case. This behavior arises because the SO coupling term $\mathcal{S}_{xy}$ mediates energy transfer from the stronger field $\bar{E}_y$ to the weaker field $\bar{E}_x$. Such intercomponent power transfer is a key manifestation of the SOI.

5. SOI Induced Structural Deformation. When the y-polarized light is odd with respect to both the x- and y-axes, the SOI induces more pronounced changes in the $\bar{E}_x$ field. To illustrate this effect, we consider the case where $\bar{E}_y$ is prepared in HG11 mode. The corresponding numerical results are shown in Fig. 5. In the absence of SOI, the nonlinearity associated with the y-polarized light generates an effective trapping potential that mirrors the HG11 profile. As $\bar{E}_x$ propagates in this potential, its spatial profile is gradually reshaped to match that of $\bar{E}_y$, as shown in Fig. 5(a).

When both nonlinearity and SOI are included, the SOI induces a noticeable beam diffraction, as shown in Fig. 5(b). The impact of the SOI is highlighted in Fig. 5(c), which shows the deviation from the nonlinearity only simulation. The diffraction also manifests in the fidelity given in Fig. 4(a2). While nonlinearity alone causes the fidelity

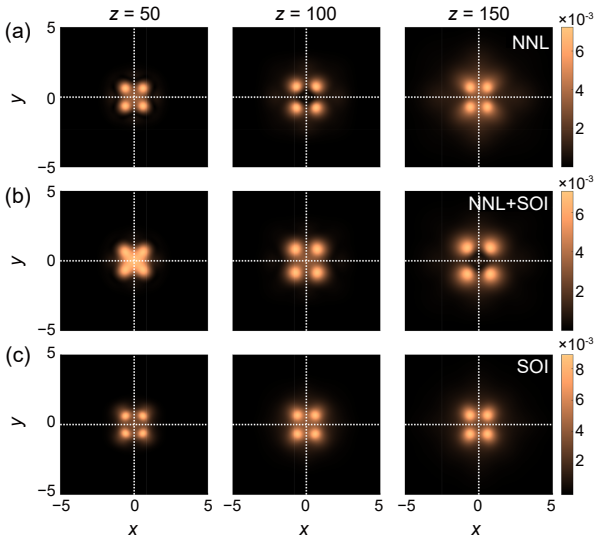

Fig. 5. Light-field amplitude $|\bar{E}_x^0|$ at different propagation distances z. The initial fields $\bar{E}_x$ and $\bar{E}_y$ are prepared in the HG00 and HG11 modes, respectively. (a) The SOI is turned off (i.e., $\mathcal{S}_{xx} = \mathcal{S}_{xy} = 0$), while (b) includes the full SOI in the simulation. Panel (c) shows the difference between the fields in (b) and (a), highlighting the SOI-induced modification of $|\bar{E}_x|$.

to decrease sharply before a partial recovery during propagation in the medium (blue curve), the inclusion of the SOI further diffuses the light field, leading to a more significant suppression of the fidelity (red dotted line).

For short propagation distances, the power variation is largely insensitive to nonlinearity, as shown in Fig. 4(b2). When the SOI is included in the simulation, the power decreases monotonically and more rapidly (red dotted line) than with nonlinearity alone. Although energy transfer between E_x and E_y occurs in both Figs. 4(b1) and 4(b2), the direction of the transfer depends on the specific symmetry and mode of the y-polarized light. This mode-dependent coupling explains the shift of the power due to the joint effects of nonlinearity and SOI, relative to the case with nonlinearity alone.

6. Conclusion. In conclusion, we have presented a theoretical investigation of light propagation in an inhomogeneous cold Rydberg gas. To account for the giant, nonlocal optical response, we develop a theoretical framework beyond the paraxial approximation. It is found that the resulting SOI is incorporated into the Helmholtz equation of the light field. A key finding of our study is that the SOI is induced by the gradients of the strong nonlocal nonlinear refractive index of the Rydberg medium, which couples the polarization and orbital motions of the light field. Based on a perturbative calculation, we further identify the scaling of the SOI with respect to the light field. We show that the SOI can be significantly amplified using elliptically polarized light consisting of one strong and one weak field. In this regime, the stronger field (e.g., the y-polarized field) amplifies the SOI effect on the weaker field (the x-polarized field). Importantly, the nonlinear SOI induces energy exchange between these strong and weak fields. The direction of this energy transfer depends on the symmetry and mode of the light fields involved. Beyond power redistribution, the SOI also leads to pronounced deformation of the transverse spatial profile during propagation, which becomes particularly significant when the strong field exhibits odd parity. Our study opens a pathway for investigating complex nonlinear light propagation that is inaccessible in linear or homogeneous media. Due to the high tunability of Rydberg interactions, in the future we can extend the study of SOI effects from the general nonlocal regime to the strongly nonlocal regime. Moreover, our study could be expanded to investigate SOI beyond the continuous-wave limit,[38] in the low-photon-number regime,[53,54] and in $\mathcal{PT}$-symmetric media.[55] In addition, our work provides a versatile platform for exploring novel optical SOI physics[56,57] in a Rydberg atom medium.

Acknowledgements. L.Q. and C.H. acknowledge the National Natural Science Foundation of China (Grant Nos. 12404377 and 12374303), the National Key Research and Development Program of China (Grant No. 2022YFA1404202), and Shanghai Municipal Science and Technology Major Project (Grant No. 2019SHZDZX01). X.Z. acknowledges the support from the Key Scientific Research Project of Colleges and Universities in Henan Province (Grant No. 26B140007) and Natural Science Foundation of Henan Province (Grant No. 252300421995). W.L. acknowledges the support from the EPSRC (Grant No. EP/W015641/1).

References

[1] Liberman V and Zel'dovich B Y 1992 *Phys. Rev. A* **46** 5199
[2] Marrucci L, Karimi E, Slussarenko S, Piccirillo B, Santamato E, Nagali E, and Sciarrino F 2011 *J. Opt.* **13** 064001
[3] Dooghin A, Kundikova N, Liberman V, and Zel'dovich B Y 1992 *Phys. Rev. A* **45** 8204
[4] Savchencko A Y and Zel'dovich B Y 1996 *J. Opt. Soc. Am. B* **13** 273
[5] Liberman V and Zel'dovich B Y 1994 *Phys. Rev. E* **49** 2389
[6] Savchenko A Y and Zel'dovich B Y 1994 *Phys. Rev. E* **50** 2287
[7] Zhang X, Hu Y, Zhou S, Zeng Z, Liu G, Lin H, Li Z, Chen Z, and Fu S 2025 *Nat. Commun.* **16** 6434
[8] Onoda M, Murakami S, and Nagaosa N 2004 *Phys. Rev. Lett.* **93** 083901
[9] Bliokh K Y and Bliokh Y P 2006 *Phys. Rev. Lett.* **96** 073903
[10] Aiello A, Lindlein N, Marquardt C, and Leuchs G 2009 *Phys. Rev. Lett.* **103** 100401
[11] Ling X, Zhou X, Huang K, Liu Y, Qiu C W, Luo H, and Wen S 2017 *Rep. Prog. Phys.* **80** 066401
[12] Kim M, Yang Y, Lee D, Kim Y, Kim H, and Rho J 2023 *Laser Photon. Rev.* **17** 2200046
[13] Nalitov A V, Malpuech G, Terças H, and Solnyshkov D D 2015 *Phys. Rev. Lett.* **114** 026803
[14] Carlini F and Cherroret N 2023 *SciPost Phys.* **14** 104
[15] Hosten O and Kwiat P 2008 *Science* **319** 787
[16] Gorodetski Y, Bliokh K Y, Stein B, Genet C, Shitrit N, Kleiner V, Hasman E, and Ebbesen T W 2012 *Phys. Rev. Lett.* **109** 013901
[17] Haefner D, Sukhov S, and Dogariu A 2009 *Phys. Rev. Lett.* **102** 123903

[18] Ciattoni A, Di Porto P, Crosignani B, and Yariv A 2000 *J. Opt. Soc. Am. B* **17** 809
[19] Bliokh K Y 2009 *J. Opt. A: Pure Appl. Opt.* **11** 094009
[20] Cardano F and Marrucci L 2015 *Nat. Photon.* **9** 776
[21] Bliokh K Y, Rodríguez-Fortuño F J, Nori F, and Zayats A V 2015 *Nat. Photon.* **9** 796
[22] Martone G I and Cherroret N 2023 *Phys. Rev. Lett.* **131** 013803
[23] Martone G I, Bienaimé T, and Cherroret N 2021 *Phys. Rev. A* **104** 013510
[24] Sodha M S and Ghatak A K 1977 *Inhomogeneous Optical Waveguides* (New York: Plenum Press)
[25] Terças H, Flayac H, Solnyshkov D D, and Malpuech G 2014 *Phys. Rev. Lett.* **112** 066402
[26] Zhang Z, Liang S, Li F, Ning S, Li Y, Malpuech G, Zhang Y, Xiao M, and Solnyshkov D 2020 *Optica* **7** 455
[27] Othonos A, Kalli K, and Kohnke G E 2000 *Phys. Today* **53** 61
[28] Yariv A and Yeh P 2007 *Photonics: Optical Electronics in Modern Communications* (Oxford: Oxford University Press)
[29] Fu S, Guo C, Liu G, Li Y, Yin H, Li Z, and Chen Z 2019 *Phys. Rev. Lett.* **123** 243904
[30] Zhao Y, Shapiro D, Mcgloin D, Chiu D T, and Marchesini S 2009 *Opt. Express* **17** 23316
[31] Cherroret N 2018 *Phys. Rev. A* **98** 013805
[32] Bardon-brun T, Delande D, and Cherroret N 2019 *Phys. Rev. Lett.* **123** 043901
[33] Wu J, Zhang J, Zhu S, and Agarwal G S 2020 *Opt. Lett.* **45** 149
[34] Abbas M, Zhang P, and Hamedi H R 2025 *Phys. Rev. A* **111** 043708
[35] Saffman M, Walker T G, and Mølmer K 2010 *Rev. Mod. Phys.* **82** 2313
[36] Shao X Q, Su S L, Li L, Nath R, Wu J H, and Li W 2024 *Appl. Phys. Rev.* **11** 031320
[37] Gorshkov A V, Otterbach J, Fleischhauer M, Pohl T, and Lukin M D 2011 *Phys. Rev. Lett.* **107** 133602
[38] Bai Z, Li W, and Huang G 2019 *Optica* **6** 309
[39] Qin L, Hang C, and Huang G 2020 *Phys. Rev. A* **102** 063707
[40] Pritchard J D, Weatherill K J, and Adams C S 2013 *Nonlinear Optics Using Cold Rydberg Atoms* (Singapore: World Scientific) p. 301
[41] Bai Z and Huang G 2016 *Opt. Express* **24** 4442
[42] Zhou L, Lu J, Zhou D L, and Sun C P 2008 *Phys. Rev. A* **77** 023816
[43] Sevinçli S, Henkel N, Ates C, and Pohl T 2011 *Phys. Rev. Lett.* **107** 153001
[44] Shi Z, Qin L, Badshah F, Zhou Y, and Huang H 2023 *Phys. Rev. A* **108** 063317
[45] Zhang X, Dunning F B, Yoshida S, and Burgdörfer J 2015 *Phys. Rev. A* **92** 051402
[46] Mohapatra A K, Bason M G, Butscher B, Weatherill K J, and Adams C S 2008 *Nat. Phys.* **4** 890
[47] Fleischhauer M, Imamoglu A, and Marangos J P 2005 *Rev. Mod. Phys.* **77** 633
[48] Zhu C, Deng L, and Hagley E 2013 *Phys. Rev. A* **88** 013841
[49] Zhu C, Deng L, Hagley E W, and Ge M L 2013 *Phys. Rev. A* **88** 045804
[50] Sun Q, Rostovtsev Y V, and Zubairy M S 2006 *Phys. Rev. A* **74** 033819
[51] Gorshkov A V, Otterbach J, Fleischhauer M, Pohl T, and Lukin M D 2011 *Phys. Rev. Lett.* **107** 133602
[52] Hang C, Bai Z, Li W, Kamchatnov A M, and Huang G 2023 *Phys. Rev. A* **107** 033503
[53] Busche H, Huillery P, Ball S W, Ilieva T, Jones M P A, and Adams C S 2017 *Nat. Phys.* **13** 655
[54] Liao R, Song Z R, Ye G S, Yu J H, Chang Y, and Li L 2025 *Phys. Rev. Lett.* **135** 260803
[55] Hang C and Huang G 2025 *Adv. Phys.* **74** 97
[56] Fu T, Lin J, Xu Y, Jia J, Wang Y, Zhang S, and Xu H 2024 *Nano Lett.* **24** 10783
[57] Puentes G 2024 *J. Eur. Opt. Society-Rapid Publ.* **20** 16